JOURNAL OF VIROLOGY, July 2010, p. 6894–6898 Vol. 84, No. 13
0022-538X/10/$12.00 doi:10.1128/JVI.00752-10

Exchange of the Coronavirus Replicase Polyprotein Cleavage Sites Alters Protease Specificity and Processing▽

Mark J. Gadlage[2,3] and Mark R. Denison[1,2,3,4]*

Departments of Pediatrics[1] and Microbiology and Immunology,[2] the Elizabeth B. Lamb Center for Pediatric Research,[3] and the Monroe Carell Jr. Children's Hospital,[4] Vanderbilt University Medical Center, Nashville, Tennessee

Received 8 April 2010/Accepted 19 April 2010

Coronavirus nonstructural proteins 1 to 3 are processed by one or two papain-like proteases (PLP1 and PLP2) at specific cleavage sites (CS1 to -3). Murine hepatitis virus (MHV) PLP2 and orthologs recognize and cleave at a position following a p4-Leu-X-Gly-Gly-p1 tetrapeptide, but it is unknown whether these residues are sufficient to result in processing by PLP2 at sites normally cleaved by PLP1. We demonstrate that exchange of CS1 and/or CS2 with the CS3 p4-p1 amino acids in engineered MHV mutants switches specificity from PLP1 to PLP2 at CS2, but not at CS1, and results in altered protein processing and virus replication. Thus, the p4-p1 residues are necessary for PLP2 processing but require a specific protein or cleavage site context for optimal PLP recognition and cleavage.

Coronaviruses are positive-strand RNA viruses that translate their first open reading frames (ORF1a and ORF1b) into polyproteins that are processed by viral proteases into intermediate and mature nonstructural proteins (nsp1 to -16) (Fig. 1A) (4, 7, 17, 20). nsp1, -2, and -3 are liberated at cleavage sites (CSs) between nsp1-2 (CS1), nsp2-3 (CS2), and nsp3-4 (CS3) by one or two papain-like protease (PLP) activities encoded within nsp3 (1, 2, 12, 13, 15) (Fig. 1B). Murine hepatitis virus (MHV) and human coronavirus 229E (HCoV-229E) use two PLPs (PLP1 and PLP2) to process at CS1 to -3, while severe acute respiratory syndrome coronavirus (SARS-CoV) and avian infectious bronchitis virus (IBV) use a single PLP each (PLpro and PLP2, respectively) (10, 20, 25, 26). The factors determining the evolution and use of one versus two PLPs by different coronaviruses for processing of nsp1, -2, and -3 are unknown. Mutations at MHV CSs or within PLP1 alter replication and protein processing in surprising ways (8, 13). Loss of processing at MHV CS1 and CS2 by CS deletion or mutation results in changes in the timing and extent of virus replication. Inactivation of MHV PLP1 is more detrimental for virus replication than deletion of CS1 and CS2 or than inactivation of PLP1 combined with the CS deletions, even though not all of the mutant viruses process at CS1 or CS2 or display similar protein processing phenotypes. In contrast to MHV results, the HCoV-229E PLP1 and PLP2 have both been shown to process at CS1 and CS2, albeit at different efficiencies (Fig. 1B) (24). Finally, the single SARS-CoV PLP2 homolog (PLpro) mediates efficient processing at CS1 to -3, each of which has an upstream position 4-Leu-X-Gly-Gly-position 1 (p4-LXGG-p1) amino acid motif implicated in PLpro processing (10, 16, 18). MHV possesses a p4-LXGG-p1 sequence only at CS3 and is cleaved by PLP2. These results suggest that p4-LXGG-p1 may be the critical determinant of recognition by PLP2/PLpro, but this hypothesis has not been tested in studies of replicating virus. Thus, it remains unknown whether the differences in PLP/CS recognition and processing are determined by the proximal p4-p1 residues (22).

In this study, we used MHV as a model to test whether PLP/CS specificities could be switched by an exchange of CS amino acid sequences and to determine the impact of CS exchange on protein processing and virus replication. Replacement of the CS3 p4-LKGG-p1 at CS2, but not at CS1, was sufficient for a switch in protease specificity from PLP1 to PLP2. Some combinations of CS exchange could not be recovered with inactive PLP1, and recovered mutant viruses had altered protein processing and/or impaired growth compared to the wild type (WT). The results confirm that p4-LXGG-p1 amino acid sequences are necessary determinants of cleavage by PLP2 but also indicate that a larger cleavage site or a different protein context is required for efficient recognition and processing. Finally, the results support the conclusion that complex relationships with respect to the timing and extent of PLP/CS interactions are essential for successful replication and, likely, for virus fitness.

Generation of CS replacement viruses. To determine the effects of alterations in PLP/CS interactions, mutations were engineered in the MHV genome that resulted in replacements of CS1 and/or CS2 by the CS3 p4-LKGG-p1 amino acid sequence in the presence of active PLP1 or inactive PLP1 (P1ko) (Fig. 1C) (6, 8, 23). Infectious virus was recovered from mutant genomes CS1(3), CS2(3), CS1/2(3), and CS1/2(3)+P1ko. Virus stocks of all recovered mutant viruses at passage 1 retained the engineered mutations, and no other mutations were identified within 300 nucleotides flanking each side of the cleavage site. The CS1/2(3)+P1ko mutant virus also retained the introduced P1ko C1121A/T1122A substitutions (8). In contrast, CS1(3)+P1ko and CS2(3)+P1ko mutant viruses could not be recovered following multiple attempts. Thus, the P1ko could be recovered only with both CS1(3) and CS2(3) exchange. This outcome is consistent with the results of our previous study, in which P1ko was recovered in combination with CS1 and CS2 deletion (ΔCS1/ΔCS2) but the presence of P1ko was highly detrimental in the presence of

* Corresponding author. Mailing address: Department of Pediatrics, Vanderbilt University Medical Center, D6217 MCN, 1161 21st Ave. S., Nashville, TN 37232-2581. Phone: (615) 343-9881. Fax: (615) 343-9723. E-mail: mark.denison@vanderbilt.edu.

▽ Published ahead of print on 28 April 2010.

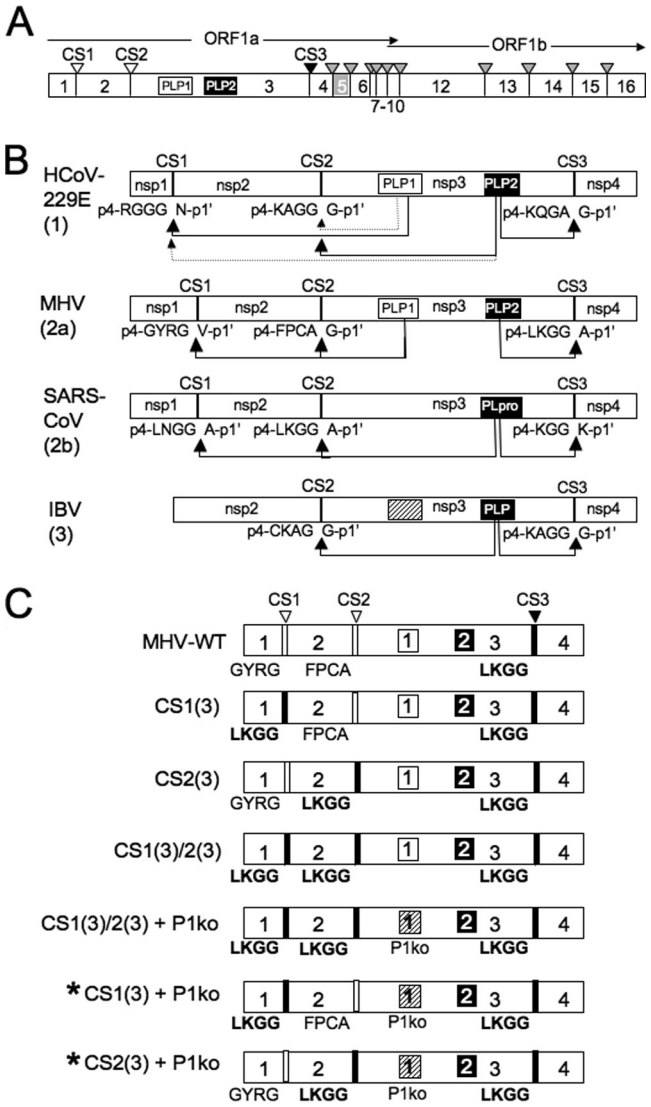

FIG. 1. MHV replicase organization, coronavirus PLP-mediated processing, and experimental design of cleavage site replacement viruses. (A) ORF1 of MHV genome RNA is shown, with overlapping ORF1a and ORF1b. The ORF1ab polyprotein is shown with nonstructural proteins (nsp1 to -16) indicated by vertical lines and numbers. Viral papain-like protease domains in nsp3 are shown as a white box containing black letters (PLP1) and a black box containing white letters (PLP2), and the nsp5 protease (3CLpro) is indicated as a gray box with a white number. Cleavage sites for PLP1 (CS1 and CS2 [shown as white arrowheads]), PLP2 (CS3 [shown as a black arrowhead]), and nsp5 (CS4 to -14 [shown as gray arrowheads]) are indicated. (B) The organization of nsp1 to nsp4 is shown for representative coronaviruses. PLPs are indicated, with the hatched box in IBV indicating a probable catalytically inactive remnant of PLP1. Processing events that were confirmed as occurring *in vitro* or during infection are shown by arrows with solid lines and large arrowheads, indicating single or dominant protease activity. The dashed lines and small arrowheads indicate minor or secondary cleavage activities. The CS amino acid sequences from position 4 (p4) to p1′ are shown for each CS, with a space and arrow representing the site of proteolytic processing. (C) The CS substitution viruses were engineered to replace the original CS amino acid sequences at CS1 and/or CS2 with that of the CS3 amino acid sequence p4-LKGG-p1. Both CS substitutions were also engineered into a catalytically inactive PLP1 (P1ko) background. PLPs are shown as numbers in boxes within nsp3. Engineered catalytically inactivated PLP1 is shown as a hatched box. Arrowheads indicate cleavage events of the WT virus and are linked to the enzyme predicted to mediate processing at the CS, as indicated by white boxes containing black characters (PLP1) or black boxes containing white characters (PLP2). The p4 through p1 amino acid residues for each CS are shown below each diagram. White and black vertical bars show the respective predicted PLP1 and PLP2 cleavage sites. Engineered substitutions are indicated in bold characters. Asterisks indicate engineered mutant genomes that could not be recovered as infectious virus.

intact CS1 and CS2, and supports a model proposing that interaction of inactive P1ko with intact CS1 and/or CS2 alters overall protein folding and impairs functions of nsp1, -2, and -3 during virus replication (8).

Polyprotein processing and growth of CS1(3) and CS2(3) viruses. To determine the effects of the CS1(3) or CS2(3) replacement on processing of nsp1, -2, and -3, cytoplasmic lysates of radiolabeled mock-, WT-, or mutant virus-infected cells were immunoprecipitated with antibodies against nsp1, nsp2, and nsp3 as well as nsp5 (3Clpro)-processed nsp8 (Fig. 2A and B) (3, 5, 9, 19, 21). The CS1(3) and CS2(3) mutants were compared with the previously characterized ΔCS1 and ΔCS2 viruses that lack the p2-p1′ CS residues and consequently have no processing at the deleted sites (8, 9). For WT and the CS2(3) mutant viruses, nsp8 was detected at equivalent levels, suggesting similar replicase polyprotein translation processes and demonstrating that the nsp5-protease function is intact (6). nsp1, nsp2, and nsp3 were also detected as mature proteins, as was the known nsp2-3 precursor (Fig. 2A and 2B) (8, 9). However, compared to WT virus, the CS2(3) mutant virus demonstrated increased levels of uncleaved nsp2-3 and decreased mature nsp2. The processing pattern of CS2(3) also differed from that of the ΔCS2 virus in which no mature nsp2 or nsp3 was detected, as was expected based on ablated processing between nsp2 and nsp3 (8). Thus, the CS2(3) virus appeared to have intact processing at the native CS1 and also at the substituted CS2(3) p4-LKGG-p1 cleavage site, albeit at a reduced efficiency compared to that seen with WT CS2. In contrast, the processing pattern of the CS1(3) virus was similar to that of the ΔCS1 virus but distinct from that of WT, with mature nsp3 but no nsp1 or nsp2 detected and with detectable nsp1-2 and nsp1-2-3 precursors. Therefore, processing appeared to be intact at the native CS2 but absent at CS1(3), suggesting that the substituted p4-LKGG-p1 amino acid sequence was not sufficient for processing of CS1(3) by PLP1 or PLP2.

We next determined whether alterations in protein processing by the CS1(3) and CS2(3) mutant viruses were associated with changes in virus replication (Fig. 2C to F). The CS2(3) mutant virus grew with kinetics and a peak titer indistinguishable from those of WT during both single-cycle and multiple-cycle infections of DBT cells, indicating that replacement of the CS2 p4-FPCA-p1 by CS3 p4-LKGG-p1 supported WT-like growth in culture, even though processing at CS2(3) took place at a lower level than at the native CS2 (Fig. 2E and F) (8). The CS1(3) virus demonstrated growth kinetics intermediate between those of the WT and ΔCS1 mutant viruses (Fig. 2C and D). This result was surprising, since there was no detectable processing at CS1(3), and we therefore predicted that the mutant virus would demonstrate the same impaired growth

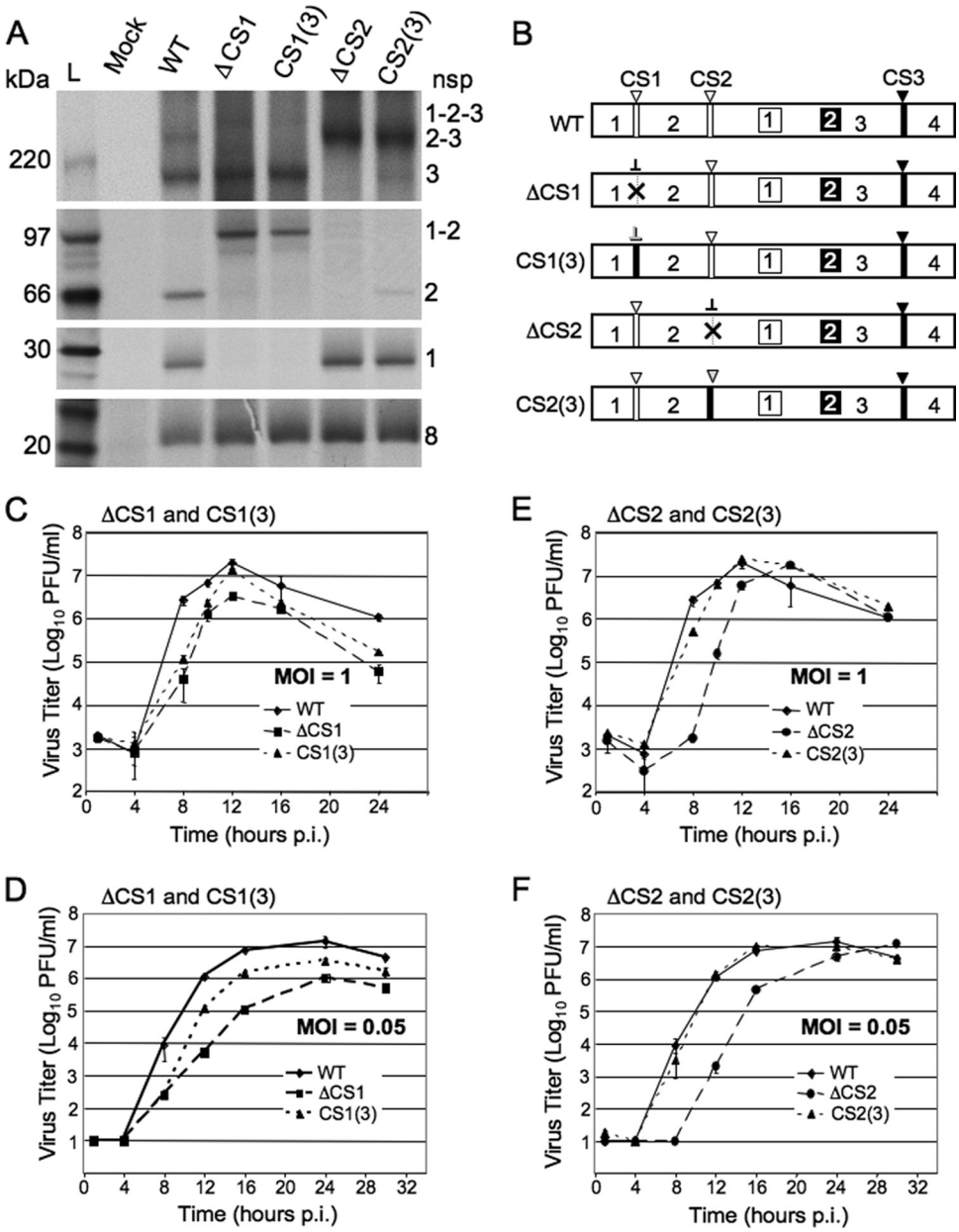

FIG. 2. Protein processing and growth of single CS substitution viruses. (A) Lysates from radiolabeled infected DBT cells were immunoprecipitated with antibodies against nsp1, nsp2, nsp3, or nsp8 as indicated, and proteins were resolved on a 4-to-12% SDS-PAGE gel and imaged by fluorography. nsp8 was used to test nsp5 (3CLpro) catalytic activity. Mature proteins (nsp1, -2, -3, and -8), known intermediate proteins (nsp2-3), and noncleaved proteins (nsp1-2-3 and nsp1-2) are indicated at the right of the gels, with molecular mass markers at the left (L). Mock, mock-infected cells. All images were obtained from a single experiment with separate gels for nsp1, -2, -3, and -8 immunoprecipitations (IP) using identical lysate concentrations, IP conditions, and imaging procedures. (B) Schematics show patterns of WT and mutant virus protein processing from the results represented in panel A. Mutations that were introduced into mutant viruses, cleavage sites, p4-p1 residues, and PLPs are as shown in Fig. 1. X's and vertical dashed lines indicate CS deletions where the p2 through p1′ amino acids were deleted. A gray-filled arrowhead indicates reduced cleavage and protease not determined. A black ⊥ symbol indicates no cleavage. A gray ⊥ symbol indicates possible but nondetected cleavage. (C to F) DBT cells were infected with the indicated viruses for single-cycle growth (multiplicity of infection [MOI] = 1 PFU/cell) or multiple-cycle growth (MOI = 0.05 PFU/cell), and titers were determined by plaque assay (14). Samples of virus supernatants were collected at the indicated time points between 1 h and 30 h postinfection (p.i.). (C) Single-cycle growth of ΔCS1 and CS1(3). (D) Multiple-cycle growth of ΔCS1 and CS1(3). (E) Single-cycle growth of ΔCS2 and CS2(3). (F) Multiple-cycle growth of the ΔCS2 and CS2(3) viruses. Data points indicate the times when media from infected cells were removed to determine titers. Error bars represent standard deviations of the results of two replicate experiments and of two measurements from each experiment.

phenotype as ΔCS1. The growth of CS1(3) virus suggests the possibility that there is processing at CS1(3) below the level of detection by immunoprecipitation or, alternatively, that substitution of p4-LKGG-p1 independently compensates for loss of cleavage at that site.

PLP2 processes at CS2(3) but not CS1(3). Since both PLP1 and PLP2 were present in the CS1(3) and CS2(3) mutant viruses, the details of protease processing at the altered cleavage sites could not be determined. To test whether PLP1 or PLP2 or both were active at altered cleavage sites, we com-

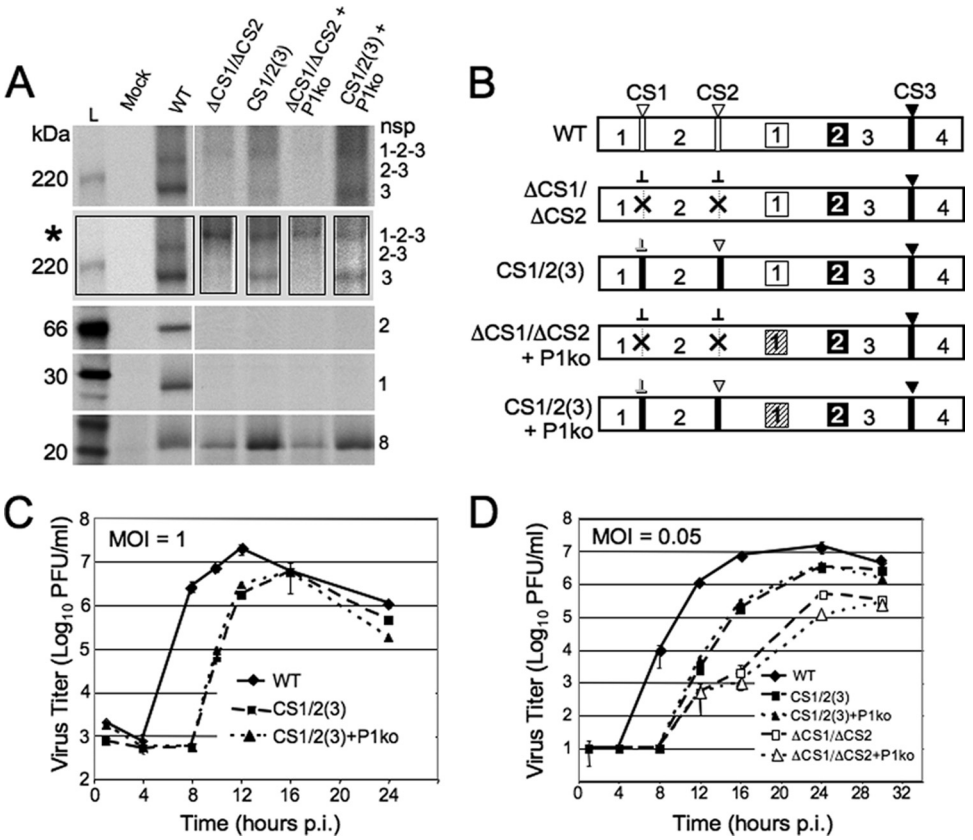

FIG. 3. Protein processing and growth analysis of the double-CS-substitution viruses. (A) DBT cells were either mock infected or infected with the viruses indicated above the gels. Cells were grown in the absence of Met and Cys for 1 h starting at 5 h postinfection (p.i.), and proteins were radiolabeled for WT infection and mutant virus infections for times that would allow optimal detection of the proteins of interest. Cell lysates were immunoprecipitated with antibodies specific for nsp1, nsp2, nsp3, or nsp8 and resolved on 4-to-12% SDS-PAGE gels. The mature, intermediate, and fusion proteins are indicated at the right of the gels. A molecular mass ladder (L) is at the left of the gel. The experiments represented by panel A were performed and imaged as described for Fig. 2. Modifications were performed equivalently for all lanes except as otherwise indicated. The panel indicated with an asterisk is the same image as in the top panel but with images in boxed rectangles individually modified by brightness and contrast to result in similar densities of nsp3 or nsp1-2-3 in order to allow visualization and comparison of relative protein amounts. (B) Schematics are shown of WT and mutant viruses used in the protein processing and growth experiments represented in the figure. The notation for the schematics is identical to that used for Fig. 1 and 2. (C and D) DBT cells were infected with either WT or double-CS-substitution viruses for growth analysis. Samples of virus supernatants were collected at predetermined time points between 1 and 30 h p.i. (C) Single-cycle growth (MOI = 1 PFU/cell). (D) Multiple-cycle growth (MOI = 0.05 PFU/cell). Data points represent the titers from media harvested at the indicated time points. The double-CS-substitution viruses and their CS deletion counterparts are linked in boxes and triangles with identical dashed lines for clarity. Error bars represent standard deviations of the means of the results obtained with the different samples.

pared protein processing of the CS1/2(3) and CS1/2(3)+P1ko mutant viruses with that of the WT, ΔCS1/2, and ΔCS1/2+P1ko viruses (Fig. 3) (8). Infection with WT virus resulted in detectable mature nsp1, -2, -3, and -8, in addition to the known nsp2-3 precursor. During infections with all mutant viruses, nsp1, -2, and -3 proteins and precursors were either not detected or detected in much lower abundance in relation to the nsp5-processed nsp8, even with extended metabolic labeling and exposure times for increased detection (Fig. 3A and B). The ΔCS1/2 and ΔCS1/2+P1ko viruses had no detectable nsp1, -2, -3, or -2-3 but did have detectable nsp1-2-3, as expected based on the abolishment of CS1 and CS2. In contrast, the CS1/2(3) and CS1/2(3)+P1ko viruses had identical patterns, with detectable nsp1-2-3 and nsp3 but no detectable nsp1, -2, or -2-3. The results demonstrate that cleavage of CS2(3), but not CS1(3), can occur in the setting of inactive PLP1, thereby implicating PLP2 in processing at the engineered CS2(3).

We next compared the growth characteristics of WT, CS1/2(3), CS1/2(3)+P1ko, ΔCS1/2, and ΔCS1/2+P1ko viruses (Fig. 3C and D). The CS1/2(3) and CS1/2(3)+P1ko mutant viruses exhibited identical levels of growth, indicating that inactivation of PLP1 was not important in the growth of the viruses and supporting the conclusion that PLP2 is the active protease at the CS2(3) site. It was interesting that both CS1/2(3) and CS1/2(3)+P1ko viruses showed a 4-h delay in exponential growth, a result similar to that seen with the ΔCS2 virus, while the CS2(3) virus alone did not (Fig. 2F), suggesting that the processing at CS2(3) may have differed in timing in the setting of altered CS1, resulting in the characteristic delay of exponential growth in the setting of impaired or abolished nsp2-3 processing. On the other hand, both CS1/2(3) and CS1/2(3)+P1ko viruses had peak virus titers that approached WT titers and were higher than the titers seen with the ΔCS1/2 and ΔCS1/2+P1ko mutants. The titer was similar to the CS1(3) virus titers and greater than the ΔCS1 virus titers, supporting

the conclusion that the p4-LKGG-p1 sequence of CS1(3) either compensates for the growth defect of loss of CS1(3) processing or, alternatively, allows processing at levels below those permitting detection by immunoprecipitation.

Discussion and conclusions. In this report, we have demonstrated that introduction of the CS3 p4-LKGG-p1 at CS2 results in a change of the effector protease from PLP1 to PLP2, whereas the same exchange at CS1 results in no processing by PLP2 as well as in loss of processing by PLP1. Thus, it appears that p4-p1 residues are necessary but not sufficient for recognition by PLP1 and PLP2. The demonstration that viable mutants were recovered with P1ko in combination with both CS1(3) and CS2(3), but not with P1ko and either CS1(3) or CS2(3) alone, extends our previous observation that P1ko was much more debilitating when introduced alone than when introduced in combination with deletion of both CS1 and CS2 (8). Further, the growth phenotypes of the CS1(3) and CS2(3) mutants were not predictable on the basis of the results seen with ΔCS1 and ΔCS2 viruses, suggesting that the presence or loss of cleavage alone was not the sole determinant of protein or precursor functions. The presence of two PLPs in some coronaviruses has been proposed to be the result of a paralogous duplication and subsequent evolution of the PLP2-like protease (26). Our results suggest that this involved more than simple protease duplication and cleavage site modification but rather may have required evolution of the entire nsp1, -2, and -3 domains and the included proteases and cleavage sites as a cassette or network of highly linked proteins and functions. If so, it is possible that nsp1, -2, and -3 may be resistant to recombination with distantly related viruses or that any viable recombination event might require exchange of the entire nsp1, -2, and -3 sequence. The independent evolutions of nsp1, -2, and -3 might also explain the significant variations in sequence and organization within nsp1, -2, and -3 between coronaviruses, in contrast to the much greater degree of conservation of sequence and organization of nsp4 to -16. Finally, the results would suggest the possibility that nsp1, -2, and -3 are more adaptable for change over time, a possibility supported by the increased mutation frequency in nsp1, -2, and -3 during the SARS-CoV epidemic compared to nsp4 to -16 (11). The panel of viruses generated in this study will provide powerful tools to study the evolution of coronavirus nsp1, -2, and -3.

We thank Michelle Becker, Lance Eckerle, Rachel Graham, Xiaotao Lu, and Jennifer Sparks for technical assistance and critical reviews of the manuscript.

This work was supported by NIH grant AI26603 (M.R.D.) from the National Institute of Allergy and Infectious Diseases. M.J.G. was supported by the Training Grant in Mechanisms of Vascular Disease through the Vanderbilt University School of Medicine (T32 HL007751). This work was also supported by the Elizabeth B. Lamb Center for Pediatric Research.

REFERENCES

1. **Bonilla, P. J., S. A. Hughes, J. D. Pinon, and S. R. Weiss.** 1995. Characterization of the leader papain-like proteinase of MHV-A59: identification of a new in vitro cleavage site. Virology **209:**489–497.
2. **Bonilla, P. J., S. A. Hughes, and S. R. Weiss.** 1997. Characterization of a second cleavage site and demonstration of activity in *trans* by the papain-like proteinase of the murine coronavirus mouse hepatitis virus strain A59. J. Virol. **71:**900–909.
3. **Bost, A. G., R. H. Carnahan, X. T. Lu, and M. R. Denison.** 2000. Four proteins processed from the replicase gene polyprotein of mouse hepatitis virus colocalize in the cell periphery and adjacent to sites of virion assembly. J. Virol. **74:**3379–3387.
4. **Brierley, I., P. Digard, and S. C. Inglis.** 1989. Characterization of an efficient coronavirus ribosomal frameshift signal: requirement for an RNA pseudoknot. Cell **57:**537–547.
5. **Brockway, S. M., X. T. Lu, T. R. Peters, T. S. Dermody, and M. R. Denison.** 2004. Intracellular localization and protein interactions of the gene 1 protein p28 during mouse hepatitis virus replication. J. Virol. **78:**11551–11562.
6. **Denison, M. R., B. Yount, S. M. Brockway, R. L. Graham, A. C. Sims, X. Lu, and R. S. Baric.** 2004. Cleavage between replicase proteins p28 and p65 of mouse hepatitis virus is not required for virus replication. J. Virol. **78:**5957–5965.
7. **Gorbalenya, A. E., E. V. Koonin, A. P. Donchenko, and V. M. Blinov.** 1989. Coronavirus genome: prediction of putative functional domains in the nonstructural polyprotein by comparative amino acid sequence analysis. Nucleic Acids Res. **17:**4847–4861.
8. **Graham, R. L., and M. R. Denison.** 2006. Replication of murine hepatitis virus is regulated by papain-like proteinase 1 processing of nonstructural proteins 1, 2, and 3. J. Virol. **80:**11610–11620.
9. **Graham, R. L., A. C. Sims, S. M. Brockway, R. S. Baric, and M. R. Denison.** 2005. The nsp2 replicase proteins of murine hepatitis virus and severe acute respiratory syndrome coronavirus are dispensable for viral replication. J. Virol. **79:**13399–13411.
10. **Harcourt, B. H., D. Jukneliene, A. Kanjanahaluethai, J. Bechill, K. M. Severson, C. M. Smith, P. A. Rota, and S. C. Baker.** 2004. Identification of severe acute respiratory syndrome coronavirus replicase products and characterization of papain-like protease activity. J. Virol. **78:**13600–13612.
11. **Chinese SARS Molecular Epidemiology Consortium.** 2004. Molecular evolution of the SARS coronavirus during the course of the SARS epidemic in China. Science **303:**1666–1669.
12. **Herold, J., A. E. Gorbalenya, V. Thiel, B. Schelle, and S. G. Siddell.** 1998. Proteolytic processing at the amino terminus of human coronavirus 229E gene 1-encoded polyproteins: identification of a papain-like proteinase and its substrate. J. Virol. **72:**910–918.
13. **Kanjanahaluethai, A., and S. C. Baker.** 2000. Identification of mouse hepatitis virus papain-like proteinase 2 activity. J. Virol. **74:**7911–7921.
14. **Kim, J. C., R. A. Spence, P. F. Currier, X. T. Lu, and M. R. Denison.** 1995. Coronavirus protein processing and RNA synthesis is inhibited by the cysteine proteinase inhibitor e64dd. Virology **208:**1–8.
15. **Lim, K. P., L. F. Ng, and D. X. Liu.** 2000. Identification of a novel cleavage activity of the first papain-like proteinase domain encoded by open reading frame 1a of the coronavirus avian infectious bronchitis virus and characterization of the cleavage products. J. Virol. **74:**1674–1685.
16. **Lindner, H. A., N. Fotouhi-Ardakani, V. Lytvyn, P. Lachance, T. Sulea, and R. Menard.** 2005. The papain-like protease from the severe acute respiratory syndrome coronavirus is a deubiquitinating enzyme. J. Virol. **79:**15199–15208.
17. **Perlman, S., and J. Netland.** 2009. Coronaviruses post-SARS: update on replication and pathogenesis. Nat. Rev. Microbiol. **7:**439–450.
18. **Ratia, K., K. S. Saikatendu, B. D. Santarsiero, N. Barretto, S. C. Baker, R. C. Stevens, and A. D. Mesecar.** 2006. Severe acute respiratory syndrome coronavirus papain-like protease: structure of a viral deubiquitinating enzyme. Proc. Natl. Acad. Sci. U. S. A. **103:**5717–5722.
19. **Sims, A. C., J. Ostermann, and M. R. Denison.** 2000. Mouse hepatitis virus replicase proteins associate with two distinct populations of intracellular membranes. J. Virol. **74:**5647–5654.
20. **Snijder, E. J., P. J. Bredenbeek, J. C. Dobbe, V. Thiel, J. Ziebuhr, L. L. Poon, Y. Guan, M. Rozanov, W. J. Spaan, and A. E. Gorbalenya.** 2003. Unique and conserved features of genome and proteome of SARS-coronavirus, an early split-off from the coronavirus group 2 lineage. J. Mol. Biol. **331:**991–1004.
21. **Sparks, J. S., X. Lu, and M. R. Denison.** 2007. Genetic analysis of murine hepatitis virus nsp4 in virus replication. J. Virol. **81:**12554–12563.
22. **Sulea, T., H. A. Lindner, E. O. Purisima, and R. Menard.** 2006. Binding site-based classification of coronaviral papain-like proteases. Proteins **62:** 760–775.
23. **Yount, B., M. R. Denison, S. R. Weiss, and R. S. Baric.** 2002. Systematic assembly of a full-length infectious cDNA of mouse hepatitis virus strain A59. J. Virol. **76:**11065–11078.
24. **Ziebuhr, J., B. Schelle, N. Karl, E. Minskaia, S. Bayer, S. G. Siddell, A. E. Gorbalenya, and V. Thiel.** 2007. Human coronavirus 229E papain-like proteases have overlapping specificities but distinct functions in viral replication. J. Virol. **81:**3922–3932.
25. **Ziebuhr, J., E. J. Snijder, and A. E. Gorbalenya.** 2000. Virus-encoded proteinases and proteolytic processing in the Nidovirales. J. Gen. Virol. **81**(Pt. 4)**:**853–879.
26. **Ziebuhr, J., V. Thiel, and A. E. Gorbalenya.** 2001. The autocatalytic release of a putative RNA virus transcription factor from its polyprotein precursor involves two paralogous papain-like proteases that cleave the same peptide bond. J. Biol. Chem. **276:**33220–33232.